Food and Chemical Toxicology 150 (2021) 112085

Contents lists available at ScienceDirect

Food and Chemical Toxicology

journal homepage: www.elsevier.com/locate/foodchemtox

Succinate dehydrogenase inhibitors: *in silico* flux analysis and *in vivo* metabolomics investigations show no severe metabolic consequences for rats and humans

H. Kamp [a,1], J. Wahrheit [a,1], S. Stinchcombe [a], T. Walk [b], F. Stauber [a], B.v. Ravenzwaay [a,*]

[a] BASF SE, Ludwigshafen, Germany
[b] BASF Metabolome Solutions GmbH, Berlin, Germany

ARTICLE INFO

Handling Editor: Chada Reddy

Keywords:
Metabolomics
in silico
Metabolic modeling
SDHI
Mitochondria
Respiratory chain
Lactate
succinate

ABSTRACT

Succinate dehydrogenase complex II inhibitors (SDHIs) are widely used fungicides since the 1960s. Recently, based on published *in vitro* cell viability data, potential health effects via disruption of the mitochondrial respiratory chain and tricarboxylic acid cycle have been postulated in mammalian species. As primary metabolic impact of SDH inhibition, an increase in succinate, and compensatory ATP production via glycolysis resulting in excess lactate levels was hypothesized. To investigate these hypotheses, genome-scale metabolic models of *Rattus norvegicus* and *Homo sapiens* were used for an *in silico* analysis of mammalian metabolism. Moreover, plasma samples from 28-day studies with the SDHIs boscalid and fluxapyroxad were subjected to metabolome analyses, to assess *in vivo* metabolite changes induced by SDHIs.

The outcome of *in silico* analyses indicated that mammalian metabolic networks are robust and able to compensate different types of metabolic perturbation, e.g., partial or complete SDH inhibition. Additionally, the *in silico* comparison of rat and human responses suggested no noticeable differences between both species, evidencing that the rat is an appropriate testing organism for toxicity of SDHIs. Since no succinate or lactate accumulation were found in rats, such an accumulation is also not expected in humans as a result of SDHI exposure.

1. Introduction

Succinate dehydrogenase inhibitor (SDHI) fungicides have been used worldwide for over 30 years for controlling plant diseases and to overcome fungal resistance to older technologies.

The enzyme succinate dehydrogenase (SDH, or succinate ubiquinone oxidoreductase) is part of the mitochondrial electron transport chain (here termed "complex II"), as well as a component of the tricarboxylic acid (TCA) cycle (Hederstedt, 2003). SDH is involved in intermediary metabolism and energy production of eukaryotic cells and of bacteria under aerobic conditions. Moreover, SDH is important for control of the hypoxia response (Koziel and Jarmuszkiewicz, 2017). SDH couples the oxidation of succinate to fumarate (in the mitochondrial matrix) to the reduction of ubiquinone (in the mitochondrial inner membrane). SDHI pesticides belonging to the chemical class of carboxamides inhibit ubiquinone reduction by reversible binding to the ubiquinone binding site (Qp site) of the fungal SDH (Scalliet et al., 2012).

In humans, germline mutations of SDH resulting in life-long decreased enzymatic activity have been associated with accumulation of succinate and the occurrence of rare neoplasia and neurodegenerative diseases (Rasheed and Tarjan, 2018). In this context, recent concerns about the safety of SDHI agrochemical fungicides have been raised by Bénit et al. (2019). They demonstrated the potential of SDHI fungicides to inhibit the human SDH enzyme. Moreover, in skin fibroblast cell culture experiments with two SDHI fungicides, the authors observed reduced cell viability if cells were additionally deprived of glucose, pyruvate and uridine, and interpreted the reduced cell viability to reflect impaired mitochondrial function. Since cultured cells produce ATP mainly through glycolysis and not from mitochondrial oxidative phosphorylation, no evidence for impaired cell viability was observed under standard cell culture conditions with 25 mM glucose present in the cell culture medium; viability experiments carried out at more physiological glucose concentrations (ca. 5 mM) were not carried out or not reported.

* Corresponding author. BASF SECarl-Bosch-Str, 3867056, Ludwigshafen am Rhein, Germany.
E-mail address: Bennard.ravenzwaay@basf.com (B.v. Ravenzwaay).
[1] co-first authors.

https://doi.org/10.1016/j.fct.2021.112085
Received 17 December 2020; Received in revised form 5 February 2021; Accepted 16 February 2021
Available online 23 February 2021

Abbreviations

BOS	Boscalid
FLX	Fluxapyroxad
GC-MS	Gas chromatography coupled with mass spectrometry
HD	High dose
LC-MS	liquid chromatography coupled with mass spectrometry
LD	Low dose
MIE	molecular initiating event
MOA	Mode of action
SDH(I)	Succinate dehydrogenase complex II (inhibitor)

In view of the inherent limitations of cell culture experiments to study mitochondrial function under physiological conditions, animal studies may be a more reliable basis to assess if SDHI fungicide exposure cause adverse health outcomes in humans via SDH inhibition. Under physiological conditions, theoretical consequences of induced enzyme inhibition can often be circumvented or compensated by alternative metabolic pathways, thereby maintaining cell or tissue homeostasis. Therefore, such *in vivo* studies integrate all metabolic pathways that may be impacted in complete organisms versus observation of isolated effects in *in vitro* experiments that are limited in the capability to model physiological conditions at tissue and more so at organism level.

For SDHI fungicides a comprehensive set of OECD guideline compliant toxicological studies is available that forms the basis for approval by regulatory authorities. This toxicological data package includes investigation of changes for a defined set of clinical chemistry parameters (such as cholesterol, albumin, triglycerides, glucose, certain liver enzymes, etc.) in experimental animals. A comprehensive determination of endogenous metabolites (such as carbohydrates, amino acids, nucleic acids or fatty acids and their derivates) from biochemical pathways is, however, beyond the scope of regulatory studies.

A technology capable of investigating a broad range of endogenous metabolites and thus changes in the underlying biochemical pathways is metabolomics (Lindon et al., 2004; Viant et al., 2019). At BASF, we have used LC-MS- and GC-MS-based metabolomics to investigate changes in plasma metabolites induced by repeated treatment of rats over 28 days with more than 1000 toxicologically well-understood (agro-)chemicals and pharmaceuticals in standardized studies, thereof also two SDH inhibiting compounds (Boscalid and Fluxapyroxad). This comprehensive metabolomic assessment resulted in the database MetaMap®Tox which can be used to predict the toxicity of new compounds, and potentially identify toxicological modes of action based on toxicity-specific metabolic patterns. A large number of studies has demonstrated robustness and reliability of the methodology (Kamp et al., 2012a,b; Mattes et al., 2014; Mellert et al., 2011; Montoya et al., 2014; Strauss et al., 2009, 2012, van Ravenzwaay et al., 2007, 2012).

In order to explore the potential consequences of SDH inhibition on cell metabolism even further, the *in vivo* metabolome studies were complemented by an *in silico* analysis of mammalian metabolism. Genome-scale modeling of metabolism has become increasingly popular in recent years as it enables the study of metabolism and prediction of biological capabilities of a target organism at a systemic level. It has been widely used in a range of scientific, industrial and medical applications, such as microbial production of chemicals, drug discovery, and human disease studies (Gu et al., 2019).

We used recently published genome-scale reconstructions of *Rattus norvegicus* (*iRno*) and *Homo sapiens* (*iHsa*) (Blais et al., 2017) and applied constraint-based modeling (Heirendt et al., 2019). A genome-scale metabolic network reconstruction represents a standardized and structured knowledge base of all known biochemical reactions in an organism. By (1) systematically linking specific genes to the respective encoded enzymes and to the chemical reactions they catalyze, (2) mathematically describing the chemical reactions and (3) imposing genetic, physicochemical and environmental constraints, context-specific genome-scale models are created. These models can be used in combination with different constraint-based modeling methods to compute phenotypic states or biological capabilities as represented by metabolic flux distributions (Orth et al., 2010; Lewis et al., 2012). In large-scale metabolic networks, such as mammalian metabolic networks, there are more reactions than there are metabolites with the result that there is no unique solution of flux distributions; redundant metabolic pathways may generate the same phenotype. Flux variability analysis (FVA) identifies all alternative solutions by determining the feasible flux ranges (minimum and maximum fluxes) for each reaction in the network. The actual flux state can only reside within this feasible solution space.

Metabolic perturbations, such as gene knockouts, enzyme inhibitions, reaction rate limitations, alternative feeding scenarios, can be simulated *in silico* by restricting or adapting the flux through the associated reactions. Such additional constraints further shrink the computable solution space and narrow the allowable flux ranges for all reactions in the network. In our *in silico* modeling approach, we address the following questions: (1) Is the applied *in silico* approach sensitive to metabolic perturbations of the respiratory chain complex? (2) What are the universal metabolic effects of SDH inhibition on mammalian metabolism? (3) Are SDHI fungicides expected to have comparable metabolic outcomes in rats and humans or are there relevant species differences in the network structure? (4) How is the human metabolism affected by SDH inhibition when challenged additionally by glucose deprivation?

Thus, the objective of the work presented here was to characterize the metabolic changes resulting from *in vivo* exposure to the SDH inhibitors boscalid and fluxapyroxad in rats, and to compare the findings both with hypothesized metabolic changes and with effect outcomes from *in silico* metabolic network predictions in rats and humans.

2. Material and methods

The plasma metabolome was measured in 28-day repeated dose studies in Wistar rats following the administration of two SDH inhibitors (Boscalid and Fluxapyroxad) and compared to untreated controls. For each dose group, five rats per sex were fed with a diet containing the individual SDH inhibitor. The top-dose level chosen in each study reflected the 28-day maximum-tolerated dose of the SDH inhibitors. The blood samples were processed for mass spectrometry-based metabolome analysis. Both gas chromatography-mass spectrometry and liquid chromatography-MS/MS were used for broad analyte profiling of the polar and non-polar fractions of the samples. Data were normalized to the median of the metabolome data derived from (the) study control samples.

2.1. Ethics statement

The animal studies were approved by the BASF Animal Welfare Body and were performed according to the German Animal Welfare Act and EU Directive 2010/63, with the permission of the local authority, the Landesuntersuchungsamt Rheinland-Pfalz (permission numbers 23 177-07/G 07-3-001 and 23 177-07/G08-3-001). The laboratory is AAALAC (Association for Assessment and Accreditation of Laboratory Animal Care International) certified.

2.2. Animal treatment, examinations and sampling

Animal handling, compound treatment as well as clinical examinations have been described earlier (Kamp et al., 2012a,b; van Ravenzwaay et al., 2007, 2012). Briefly, Wistar rats (CrI:WI(Han)) were supplied by Charles River, Germany and were approx. 70 days old at the beginning of the studies. The diet and drinking water were available ad libitum (except before blood sampling) and regularly assayed for

chemical contaminants and the presence of micro-organisms. There were 5 animals per sex per dose group and 10 animals per sex in the control group. The animals were treated with the test compounds on a daily basis for 28 days via the diet at dose levels of 6,000 ppm (high dose, HD) and 1,000 ppm (low dose, LD) for Fluxapyroxad (FLX) and 15, 000 ppm (HD) and 5,000 ppm (LD) Boscalid in both studies (BOS-11 as well as (BOS-76). The dose levels were set based on available regulatory toxicity studies (Boscalid: FAO/WHO, 2008; Fluxapyroxad: FAO/WHO, 2013). The compounds were produced by BASF with a purity of 99.8% for FLX and 95.7% for BOS-11, as well as 99.3% for BOS-76.

All animals were checked daily for mortality and clinical signs. Food consumption was determined on study days 7, 14, 21 and 28. Body weight was determined before the start of the administration period in order to randomize the animals and on study days 0, 4, 7, 14, 21 and 28. Blood samples for metabolome analysis were taken by puncturing the retrobulbar venous plexus on study day 7, 14 and 28 from overnight fasted animals under isoflurane anesthesia and the obtained EDTA-plasma was covered with nitrogen and frozen at −80 °C. At the end of the treatment period, the animals were sacrificed by decapitation under isoflurane anesthesia.

2.3. MetaMap®Tox methodology

2.3.1. Metabolite profiling (metabolomics)

The plasma metabolome was examined by BASF metabolome solutions GmbH following proprietary sample work up using GC-MS and LC-MS/MS techniques as described in Montoya et al., 2014. Briefly, three types of mass spectrometry analysis were applied to all samples: GC-MS (gas chromatography-mass spectrometry) and LC-MS/MS (liquid chromatography-MS/MS) were used for broad profiling, as described in van Ravenzwaay et al. (2007). SPE-LC-MS/MS (Solid phase extraction-LC-MS/MS) was applied for the determination of catecholamine and steroid hormone levels. Proteins were removed from plasma samples by precipitation. Subsequently polar and non-polar fractions were separated for both GC-MS and LC-MS/MS analysis by adding water and a mixture of ethanol and dichloromethane. For GC-MS analysis, the non-polar fraction was treated with methanol under acidic conditions to yield the fatty acid methyl esters derived from both free fatty acids and hydrolyzed complex lipids. The non-polar and polar fractions were further derivatized with O-methyl-hydroxylamine hydrochloride and pyridine to convert oxo-groups to O- methyl-oximes and subsequently with a silylating agent before analysis (Roessner et al., 2000). For LC-MS analysis, both fractions were reconstituted in appropriate solvent mixtures. HPLC was performed by gradient elution using methanol/water/formic acid on reversed phase separation columns. Mass spectrometric detection technology was applied which allows target and high sensitivity MRM (Multiple Reaction Monitoring) profiling in parallel to a full screen analysis (patent application 2003073464). For all metabolites, changes were calculated as the ratio of the mean of metabolite levels in individual rats in a treatment group relative to mean of metabolite levels in rats in a matched control group (time point, dose level, sex). The methods resulted in 183 semi-quantitative analytes, 162 of which are chemically identified and 21 are structurally not elucidated.

2.3.2. The MetaMap®Tox database

MetaMap®Tox is a unique database of biochemical profiles from rat plasma and comprehensive pharmacological and toxicological data base of currently approximately 1,000 pharmaceuticals, chemicals and agrochemicals after 7, 14 and 28 days of test substance treatment. MetaMap®Tox was used to evaluate the metabolome of the test compounds in terms of number and strength of metabolite changes, comparison to specific toxicity patterns as well as correlation analysis with other reference compounds in the data base.

2.3.3. Statistics

The data were analyzed by univariate and multivariate statistical methods. The sex- and day-stratified heteroscedastic *t*-test (Welch test) was applied to log-transformed semi-quantitative metabolite data to compare treated groups with respective controls. p-values, t-values, and ratios of corresponding group medians were collected as metabolome profiles and fed into MetaMap®®Tox).

2.3.4. Pattern ranking

Discriminating metabolite patterns for various toxicological modes of action (MoAs) were developed from the metabolite profiles in the MetaMap®Tox database. These metabolite patterns are usually based on the data from at least three different reference chemicals included in the MetaMap®Tox database which share a common toxicological mode of action (van Ravenzwaay et al., 2012). The pattern ranking itself is a two-step process. Firstly, an algorithm used in the database yields a ranking list based on similarity of the test compound metabolome profile compared to the specific patterns in MetaMap®Tox using a median r value metric. Secondly, the metabolite changes are evaluated by an expert panel of experienced toxicologists to determine what may be described as “confirmed” matches. Generally, based on the number of commonly changed metabolites, a clear match prerequisites approx. 90% or more of metabolites significantly changed as defined by the pattern (weak matches: approx. 75–90%; equivocal findings: approx. 50–75%; mismatches: <50%). Furthermore, the quality and importance of the metabolite changes for a certain toxicological mode of action is considered for this evaluation.

2.3.5. Profile comparison

The profile comparisons were conducted by calculating Welch t-values from treatment and control samples of each metabolite stratified by sex and time. By a pair-wise comparison the profiles (t-values) of the two treatments in question were compared with each profile available in the MetaMap®Tox database. These comparisons were quantified by calculating the parametric Pearson product moment correlation coefficient. The similarity between the profiles of the compound under investigation and the compounds of the MetaMap®Tox database was ranked by the resulting correlation coefficients in descending order. A threshold value of 0.40 for male animals and 0.50 for female animals displays approximately the 95th percentile of all correlation coefficients obtained by the profile comparison. Correlation coefficients above these values are considered as indicating a match between two treatments (Mattes et al., 2013; van Ravenzwaay et al., 2015).

2.4. In silico analysis in genome-scale metabolic models

2.4.1. Methodology

We used recently published metabolic reconstructions of *Rattus norvegicus* (*iRno*) and *Homo sapiens (iHsa)* (Blais et al., 2017). Experimental values of the 28-day rat *in vivo* studies (explained above) were imposed as physiological constraints to convert the genome-scale reconstructions into context-specific genome-scale models. Different types of metabolic perturbation (e.g. reaction knockout) were applied as additional constraints in several *in silico* test scenarios. Flux Variability Analysis (FVA) was performed to determine the ranges of allowable flux values. Finally, the consequences of different metabolic perturbations were qualitatively analyzed by comparing the computed ranges of flux distributions between different scenarios. A schematic overview of the *in silico* methodology and analysis test design is shown in Fig. 1. Details are explained in the following text.

2.4.2. Constraint-based modeling

The COBRA (COnstraint-Based Reconstruction and Analysis) toolbox 3.0 (Heirendt et al., 2019) was used in the MATLAB (MATLAB R2019b, MathWorks) environment for constraint-based modeling. A Flux Variability Analysis (FVA) was performed to determine the flux ranges

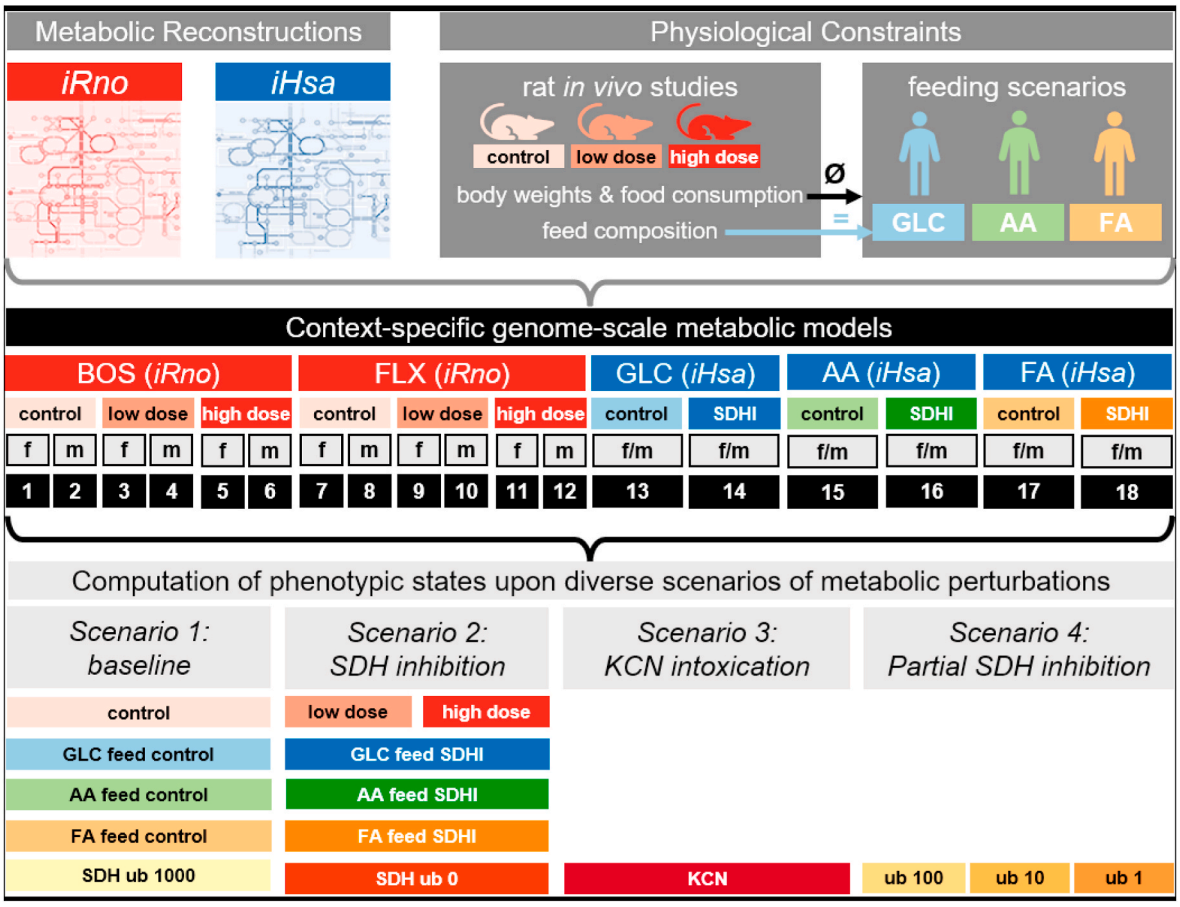

Fig. 1. Strategy for *in silico* analysis of metabolism in genome-scale models. Genome-scale network reconstructions of rat (*iRno*) and human (*iHsa*) metabolism were combined with physiological constraints from the 28-day rat *in vivo* studies (rat body weights, food consumption rates, feed composition), and additional artificial feeding scenarios simulating glucose deprivation, to create 18 different context-specific genome-scale metabolic models (see also Supplementary Table 1, Feed Constrained Models): model 1–6, representing the rat Boscalid (BOS) *in vivo* study, model 7–12, representing the rat Fluxapyroxad (FLX) *in vivo* study, and model 13–18, applied for *in silico* analyses of human metabolism in glucose (GLC), amino acid (AA), or fatty acid (FA) feeding scenarios. Genome-scale models were applied in constraint-based modeling to compute phenotypic states, described by feasible metabolic flux distributions as determined by flux variability analysis (FVA). Diverse metabolic perturbations were tested and qualitatively compared with each other in four different *in silico* scenarios: (1) baseline, upper bound (ub) of SDH flux unconstrained (1000 μmol/(g dry weight × h)), (2) (complete) SDH inhibition, ub of SDH flux set to 0 μmol/(g dry weight × h), (3) KCN (Potassium cyanide) intoxication, ub of electron transport chain complex IV flux set to 0 μmol/(g dry weight × h), and (4) partial SDH inhibition ub of SDH flux set to 1, 10, or 100 μmol/(g dry weight × h).

(minimum and maximum fluxes, [μmol/(g dry weight × h)]) which are feasible at the given constraints, according to the following COBRA function:

[minFlux, maxFlux] = fluxVariability(fvamodel, 100, 'max', rxnNameList); More detailed information on the method can be found in the COBRA toolbox manual (Heirendt et al., 2019) and in previous publications reviewing constraint-based modeling (O'Brien et al., 2015; Orth et al., 2010; Lewis et al., 2012; Price et al., 2004). Constraints are detailed in the following.

2.4.3. Integration of experimental values from 28-day in vivo rat studies as basic model inputs

Experimental values of rat body weights and food consumption from the 28-day *in vivo* studies with BOS and FLX were used to calculate weight gain rates (growth rates) [1/h] and food consumption rates [g food/(g rat dry weight × h)] for the 28-day study period (see Supplementary Table 1, Body Weights, Food Consumption, Weight Gain Rates, Feed Rates). Guidance for conversion from body weight to dry weight was taken from literature (Suckow et al., 2006). Considering a water content of rats of 68%, the dry weight was calculated as follows:

dry weight [g] = 0.32 × body weight [g]

Feed composition was taken from supplier information (KLIBA NAFAG, Maus und Ratte, 3433, GLP). Components in the feed were mapped to matching exchange reactions in the metabolic models (see Supplementary Table 1, Feed Exchange Mapping).

Upper bounds of exchange fluxes [μmol/(g dry weight × h)] were calculated from food consumption rates and feed composition. Calculation was differentiated by test compound (BOS (MoA11), FLX), dose level (control, low dose, high dose) and gender (female, male). This resulted in twelve distinct *iRno* models for *in silico* simulations of rat metabolism (see Fig. 1, model 1–12), each constrained by respective experimental values (Supplementary Table 1, Feed Constrained Models).

The human metabolic model (*iHsa*) was constrained with averaged values from the rat studies in order to apply physiological constraints at comparable orders of magnitude for both rat and human *in silico* studies. Weight gain rates and feed consumption rates were averaged for study (BOS, FLX), SDHI dose level (low dose, high dose) and gender (female, male). This resulted in two different models for human *in silico* studies (see Fig. 1, model 13 and 14) differentiated by distinct weight gain rates and food consumption per condition (control, SDHI).

2.4.4. Adaptation of feed constraints to simulate glucose deprivation

We tested if the human metabolic network can be sustained without

any glucose supply, solely fed by alternative carbon sources. For these test scenarios, we modified the feed constraints for the above described *in silico* model of human metabolism (*iHsa*) to contain no glucose as carbon source but elevated amounts of amino or fatty acids. In total, three different feeding scenarios were investigated, (1) GLC, which is equivalent to the experimental glucose containing feed (Fig. 1, model 13 and 14), (2) AA, containing no glucose, but 2.5 times more amino acids compared to experimental feed (Fig. 1, model 15 and 16), and (3) FA, containing no glucose, but 3 times more fatty acids compared to experimental feed (Fig. 1, model 17 and 18) (Supplementary Table 1, Feed Constrained Models).

2.4.5. Test scenarios for in silico simulation of succinate dehydrogenase inhibition in rat and human metabolism

In the metabolic reconstructions *iRno* and *iHsa*, the succinate dehydrogenase function is represented by two alternative reactions creating a loop if left unconstrained:

- RCR11674, succinate dehydrogenase: FADH2 + fumarate = FAD + succinate
- RCR14481, electron transport chain II: fumarate + ubiquinol = succinate + ubiquinone

2.4.5.1. Scenario 1: baseline. For comparison with SDH inhibition scenarios, baseline simulations were first performed. The reaction RCR14481 as one of the two alternative reactions was closed, i.e. no flux was allowed through this reaction by setting upper and lower bounds to zero. Only reaction RCR11674 was allowed to carry a flux, to transfer electrons and to convert fumarate into succinate. Scenario 1 as baseline simulation (avoiding circulation of carbons by an unconstrained loop) was applied to rat and human models constrained by experimental values of control groups (Fig. 1, models 1, 2, 7, 8, 13, 15, 17).

2.4.5.2. Scenario 2: succinate dehydrogenase inhibition. For *in silico* simulation of succinate dehydrogenase inhibition, both reactions, RCR11674 and RCR14481, were set to zero flux, which is equivalent to a complete inhibition or a knockout of the succinate dehydrogenase function. Scenario 2 as SDH inhibition simulation was applied to rat and human models constrained by experimental values of fungicide treated groups (Fig. 1, models 3–6, 9–12, 14, 16, 18).

2.4.5.3. Scenario 3: Potassium cyanide (KCN) intoxication vs. complete SDH inhibition. Network flexibility and robustness of mammalian metabolism was further investigated by additional scenarios testing different levels of perturbation of the respiratory chain. The metabolic effects of complete SDH inhibition, i.e. inhibition of electron transport chain complex II, were compared with the effects induced by a simulated KCN intoxication, i.e. inhibition of electron transport chain complex IV. A block of complex IV is indisputably considered a severe metabolic perturbance of mammalian metabolism. For this simulation, the reaction RCR21046 (electron transport chain IV: 8 H+ + O2 + 4 ferrocytochrome C → 2 H2O + 4 H+ + 4 ferricytochrome C) was not allowed to carry a flux.

2.4.5.4. Scenario 4: Complete vs. partial SDH inhibition (vs. baseline). Since complete inhibition of SDH is unlikely to happen in mammalian metabolism under more realistic conditions of low-level exposure to SDHI fungicides, we investigated three scenarios where the flux bounds of SDH are not set to zero, but only restricted to a flux of 1 μmol/(g dry weight × h), 10 μmol/(g dry weight × h) or 100 μmol/(g dry weight × h), representing different levels of partial SDH inhibition.

In order to avoid an influence imposed by experimental values (e.g. variable food consumption rates), all simulations of scenario 3 and 4 were applied to the same input model (Fig. 1, model 1).

3. Results

3.1. Bodyweight, food consumption and clinical findings

Neither bodyweight nor food consumption were significantly altered in male or female animals due to the treatment with high (15,000 ppm) or low dose (5,000 ppm) levels for the BOS-11 and BOS-76 groups. The test substance intake at a dose level of 15,000 ppm is roughly equivalent to 1,200 mg/kg bw, the highest dose to be tested in 28-day OECD guideline 407 studies. For FLX at day 28 of the metabolome study, body weights for high dose (6,000 ppm) males were 14% lower than the controls, food consumption was reduced by 17%. For high dose females body weights were 5% and food consumption 12% lower, respectively. No changes in body weight were observed at the low dose (1,000 ppm) in both sexes. The test substance intake at a dose level of 6,000 ppm is equivalent to 480 mg/kg bw. There were neither mortalities, nor clinical signs of toxicity observed during the whole study duration for any of the treatment groups.

3.2. In vivo metabolome assessment

3.2.1. Significant metabolite changes

In the supplementary table 2 the whole metabolome profiles of BOS-11, BOS-76 and FLX can be seen.

Both Boscalid (BOS) and Fluxapyroxad (FLX) induced strong changes in the metabolite profile of male and female animals compared to the control (number of metabolites with significant changes four to five times above the false positive rate at $p < 0.05$ of 5%). The observed effects were more moderate for female rats at FLX treatments after 7-day treatment, as well as in male rats for the low level of BOS (5,000 ppm) after seven days of treatment (three-times increase of significantly changed metabolite numbers).

Generally, for FLX and BOS, the changes found at the high dose were also observed at the low dose, however, the number of significantly changed metabolites was lower than for the high dose.

For both compounds, BOS and FLX, consistent metabolite changes are found for increased levels of fatty acids as well as more complex lipids, e.g. (lyso-)phosphatidylcholines and sphingomyelins. In a few cases there were changes in the amino acid metabolism, e.g. increased levels of serine, glycine and threonine, histidine, ornithine as well as of branched chain amino acids (valine, leucine, isoleucine). These amino acids were mostly not changed or did lack statistical significance for BOS-11. Quite consistently 2-hydroxy butyrate was found to have lower metabolite levels compared to the control. Furthermore, glucuronic acid was increased consistently for both compounds at all dose levels (Table 1).

3.2.2. Pattern evaluation

The metabolite profiles of FLX and BOS were compared with patterns available in the MetaMap®Tox database (data not shown). The assessment for both BOS treatments yielded similar results and confirmed the liver and thyroid as target organs. Matches were observed with patterns for liver enzyme induction and for indirect thyroid effects (resulting from increased excretion of thyroid hormones due to liver enzyme induction) as well as liver toxicity in both sexes. Taken together, the data for both BOS treatments demonstrate robustness and reproducibility of the metabolome evaluation.

The comparison of metabolite changes induced by FLX with the patterns in MetaMap®Tox also confirmed liver and thyroid as target organs through matches with liver enzyme induction, indirect thyroid effects (resulting from increased excretion of thyroid hormones due to liver enzyme induction), as well as liver toxicity in both sexes at the high dose treatment.

3.2.3. Treatment correlation

Based on whole metabolite profile correlation, the high dose

Table 1
Amino acid, ornithine, hydroxybutyrate and glucuronic acid changes in rats treated with FLX or BOS (bold numbers indicate a statistically significant change, whereby yellow colour indicates a statistically significant decrease, red colour a statistically significant increase at $p < 0.05$; f: female; m: male; 28 indicates the treatment period in days).

	FLX-46 HD		FLX-46 LD		BOS-11 HD		BOS-11 LD		BOS-76 HD		BOS-76 LD	
Metabolite	**f28**	**m28**	**f28**	**m28**	**f28**	**m28**	**f28**	**m28**	**f28**	**m28**	**f28**	**m28**
Glycine	**1.51**	**1.26**	1.11	**1.33**	**1.25**	**1.58**	**1.25**	1.15	**1.59**	**1.40**	**1.42**	**1.49**
Histidine	**1.84**	**1.71**	**1.30**	**1.31**	1.11	0.92	1.14	0.90	**1.84**	**1.55**	**1.54**	**1.51**
Isoleucine	**1.23**	**1.40**	**1.45**	**1.40**	0.95	**0.83**	1.05	0.92	**1.40**	**1.23**	**1.29**	**1.17**
Leucine	**1.24**	**1.54**	**1.46**	**1.41**	0.94	**0.84**	1.04	0.91	**1.58**	**1.31**	**1.39**	**1.25**
Serine	**1.36**	**1.14**	1.05	**1.13**	0.96	1.02	0.98	0.90	**1.16**	1.24	1.02	**1.26**
Threonine	**1.77**	1.36	**1.23**	**1.24**	1.09	1.06	1.12	1.02	**1.35**	1.45	**1.25**	**1.49**
Valine	**1.20**	**1.39**	**1.37**	**1.26**	0.95	**0.90**	1.01	0.99	**1.45**	**1.25**	**1.31**	**1.15**
Ornithine	**1.57**	**1.55**	**1.29**	**1.30**	0.95	1.07	1.22	1.01	**1.23**	1.36	**1.22**	**1.23**
Glucuronic acid	**9.54**	**4.99**	**3.51**	**1.74**	**2.27**	**1.48**	**2.03**	**1.42**	**2.64**	1.13	**2.05**	1.13
2-Hydroxybutyrate	1.05	1.48	**0.61**	**0.47**	**0.52**	**0.70**	**0.86**	**0.65**	**0.56**	**0.68**	**0.52**	0.90

treatments of BOS-11 and BOS-76 are most similar to each other, with a correlation coefficient of 0.737 in males and 0.697 in females. In both sexes these correlation coefficients exceed the 99th percentile of all possible correlations.

The high dose treatment of FLX with the two BOS treatments showed high similarity between FLX and BOS with correlation coefficients of 0.641 (BOS-11) and 0.668 (BOS-76) in male animals and 0.594 (BOS-11) and 0.649 (BOS-76) in female animals. All correlation coefficients exceed the 99th percentile of all possible correlations, with the exception of the comparison of FLX and BOS-11 in female animals, exceeding the 98th percentile.

3.3. SDHI-related metabolome changes

Table 2 shows the extent of tricarboxylic acid (TCA)-related metabolite changes in rats treated with FLX or BOS. There were no consistent effects of the compounds on these metabolites. Overall, the fold-changes are low, and statistical significance was obtained only in a low number of occasions. Consequently, no pattern emerged from these data. For these changes, neither a dose-response relationship, nor consistency between the sexes was observed. Furthermore, in the case of the two studies with BOS, none of the effect changes were reproducible.

3.4. In silico analysis of metabolism in genome-scale rat and human models

We applied experimental values of rat *in vivo* studies as physiological constraints to create context-specific models of rat and human metabolism. Flux variability analysis (FVA) was used to determine the minimum and maximum flux values for each reaction upon different scenarios of metabolic perturbation. Selected results of flux distributions are presented in Fig. 2. The complete set of computation results can be found in the supplementary material (see Supplementary Table 2, FVA results). If a range of possible values for a reaction rate is computed, the actual *in vivo* flux rate is predicted to be within this feasible flux range. Variable reaction rates are expected for large-scale metabolic networks due to network redundancy and the existence of alternative pathways (O'Brien et al., 2015). Reactions of phosphofructokinase (PFK), succinate ligase (SUCLG), fumarase (FHc and FHm) and mitochondrial alanine aminotransferase (ALATm) had flux values with infinite bounds (−1000, +1000) at all tested conditions (see Fig. 2). These reactions were unbounded as the applied constraints had no effect on the computed flux capacity of these reactions. However, most reactions in the intermediary metabolism were found to have variable flux values, (1) for models constrained by physiological data from male or female rats, and (2) at different conditions of metabolic perturbation; this indicates that these reactions are sensitive to the various applied constraints.

3.4.1. Complete inhibition of succinate dehydrogenase has only minor effects on rat and human metabolism

We compared the metabolic effects of a complete reaction knockout of succinate dehydrogenase (low dose or high dose for rat metabolism, SDHI for human metabolism, see Fig. 1, scenario 2) with the flux distributions obtained at baseline condition (control, see Fig. 1, scenario 1) both in rat and human metabolic models. Since previous results of Bénit

Table 2
Tricarboxylic acid (TCA)-related metabolite changes in rats treated with FLX or BOS (bold numbers indicate a statistically significant change, whereby yellow colour indicates a statistically significant decrease, red colour a statistically significant increase at $p < 0.05$; f: female; m: male; 7, 14, 28 indicate the treatment period in days).

	FLX-46 HD		FLX-46 LD		BOS-11 HD		BOS-11 LD		BOS-76 HD		BOS-76 LD	
Metabolite	**f28**	**m28**	**f28**	**m28**	**f28**	**m28**	**f28**	**m28**	**f28**	**m28**	**f28**	**m28**
Citrate	0.96	0.94	**0.74**	**0.82**	1.08	0.99	1.05	**0.90**	1.01	0.88	0.95	0.93
Lactate	0.82	1.10	1.01	1.22	1.49	0.86	1.59	**0.87**	1.08	0.75	**1.31**	0.93
Malate	0.82	1.11	1.72	1.07	0.65	**0.63**	1.10	**0.68**	1.06	0.81	0.82	0.83
Pyruvate	0.82	0.72	0.86	0.77	1.24	1.21	1.18	0.96	0.67	**0.63**	0.94	0.66
Succinate	0.94	1.02	1.02	1.04	**0.95**	0.98	0.97	1.01	1.05	0.97	1.03	0.96

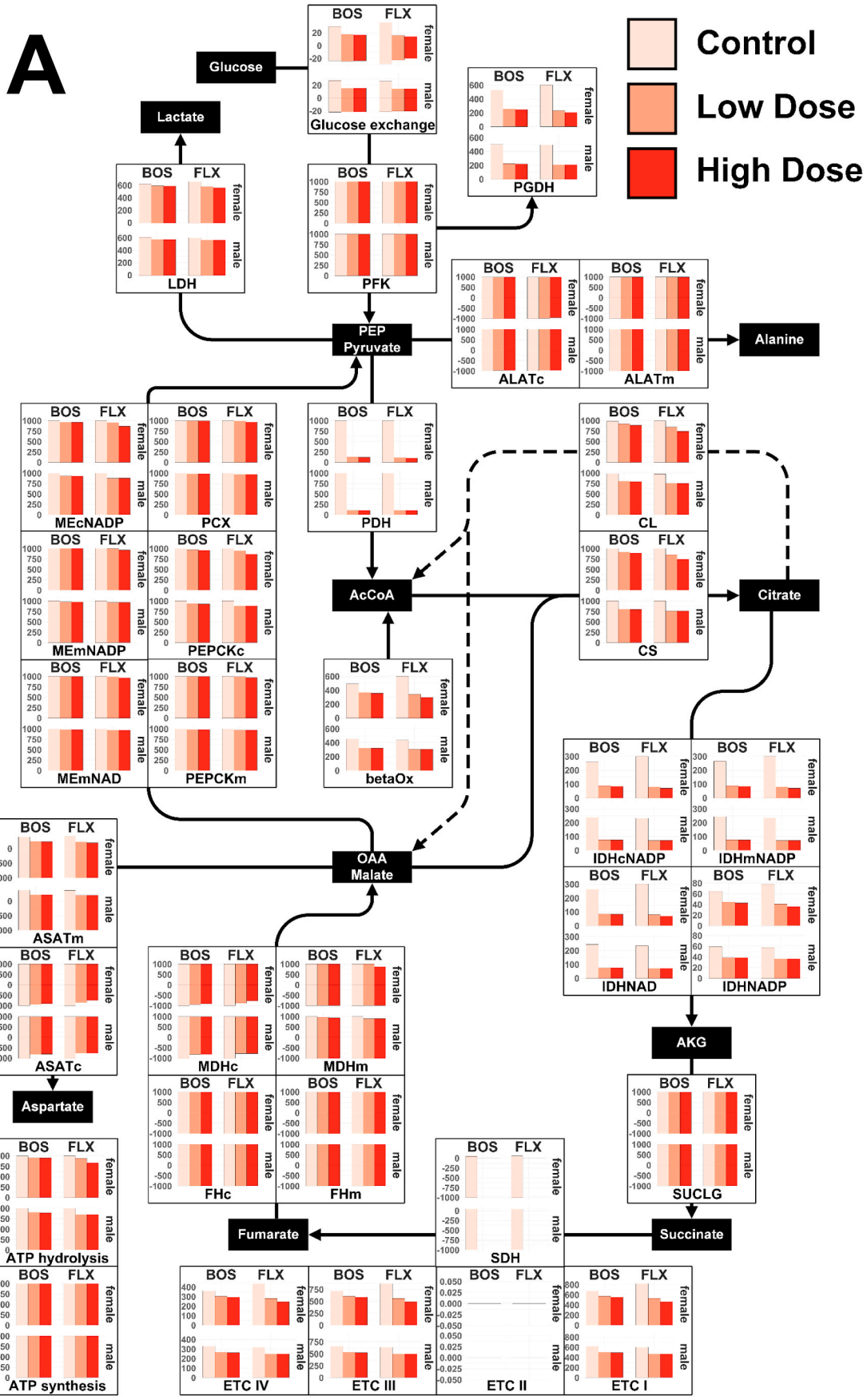
A
Control
Low Dose
High Dose
Glucose
Lactate
Glucose exchange
PGDH
LDH
PFK
PEP
Pyruvate
ALATc
ALATm
Alanine
MEcNADP
PCX
PDH
CL
MEmNADP
PEPCKc
AcCoA
Citrate
CS
MEmNAD
PEPCKm
betaOx
IDHcNADP
IDHmNADP
ASATm
OAA
Malate
IDHNAD
IDHNADP
ASATc
MDHc
MDHm
AKG
Aspartate
FHc
FHm
SUCLG
ATP hydrolysis
Fumarate
SDH
Succinate
ATP synthesis
ETC IV
ETC III
ETC II
ETC I
BOS
FLX
female
male

Fig. 2. Metabolic flux maps depicting feasible flux distributions [μmol/(g dry weight × h)] for *in silico* simulations of different metabolic perturbations. (A) BOS – Boscalid *in silico* rat study, FLX – Fluxapyroxad *in silico* rat study. Physiological constraints derived from rat *in vivo* studies. Baseline scenario 1 (control) vs. SDH inhibition scenario 2 (low dose, high dose). (B) Three different *in silico* feeding scenarios in human metabolism: GLC – Glucose feed, identical to feed composition of rat *in vivo* study, AA – Amino acid feed (amino acids of *in vivo* feed composition × 2.5, no glucose supply), FA – Fatty acid feed (fatty acids of *in vivo* feed composition × 3, no glucose supply). Physiological constraints derived from rat *in vivo* studies, averaged for SDHI fungicide compounds, SDHI fungicide dose level, and gender. Baseline scenario 1 (control) vs. SDH inhibition scenario 2 (SDHI). (C) Comparison of different *in silico* metabolic perturbations of the respiratory chain in rat metabolism. Physiological constraints of group Boscalid/control/female (Fig. 1, model 1) from rat *in vivo* studies. Baseline scenario 1 (SDH upper bound (ub) 1000) vs. partial SDH inhibitions in scenario 4 (SDH ub 100, SDH ub 10, SDH ub 1) vs. complete SDH inhibition scenario 2 (SDH ub 0) vs. KCN intoxication scenario 3 (KCN, i.e. complete inhibition of respiratory chain complex IV). Abbreviations:, BOS – Boscalid, FLX – Fluxapyroxad, GLC – Glucose, AA – Amino acid, FA – Fatty acid, SDH ub – Succinate Dehydrogenase flux upper bound, KCN - Potassium cyanide, PEP – Phosphonenolpyruvate, AcCoA – Acetyl-Coenzyme A, OAA – Oxaloacetate, AKG – Alpha-KetoglutaratePFK - Phosphofructokinase, PGDH – Phosphogluconate dehydrogenase, PDH – Pyruvate dehydrogenase, LDH – Lactate dehydrogenase, CS – Citrate synthase (Note: the Citrate synthase equation is defined in opposite direction in the metabolic reconstructions, flux results have been reversed here for easier interpretation), IDHNAD – NAD-dependent isocitrate dehydrogenase, IDHNADP - NADP-dependent isocitrate dehydrogenase, IDHmNADP - mitochondrial NADP-dependent isocitrate dehydrogenase, IDHcNADP - cytosolic NADP-dependent isocitrate dehydrogenase, SUCLG – Succinate ligase, SDH – Sucinate dehydrogenase, FHc – cytosolic fumarase, FHm – mitochondrial fumarase, MDHc – cytosolic malate dehydrogenase, MDHm – mitochondrial malate dehydrogenase, ETC I – electron transport chain complex I, ETC II – electron transport chain complex II, ETC III – electron transport chain complex III, ETC IV – electron transport chain complex IV, MEmNAD - mitochondrial NAD-dependent malic enzyme, MEmNADP- mitochondrial NADP-dependent malic enzyme, MEcNADP- cytosolic NADP-dependent malic enzyme, PEPCKc - cytosolic Phosphoenolpyruvate dehydrogenase, PEPCKm - mitochondrial Phosphoenolpyruvate dehydrogenase, PCX – Pyruvate carboxylase, ASATc – cytosolic aspartate aminotransferase, ASATm – mitochondrial aspartate aminotransferase, ALATc – cytosolic alanine aminotransferase, ALATm. – mitochondrial alanine aminotransferase, CL – citrate lyase, betaOx – beta-Oxidation (Note: shown are the flux results for the palmitoyl-CoA dehydrogenase reaction (RCR12716).

et al. suggested that fatal effects of SDHI fungicides in human cell culture are only evident if cells were also deprived of glucose, we additionally tested the metabolic capabilities of the human network at SDH inhibition without glucose supply in two different *in silico* scenarios feeding amino acids (AA feed) or fatty acids (FA feed) as alternative carbon sources instead of glucose.

Results obtained for simulations with the rat metabolic models (see Fig. 2A, BOS and FLX) and the human metabolic models (see Fig. 2B, GLC, AA, FA) were consistent and no noticeable differences were observed between both species.

Only few metabolic reactions were found to have substantially smaller flux capacities at inhibition of SDH compared to the control condition. At baseline conditions, the pyruvate dehydrogenase (PDH) reaction was unbounded (infinite value of +1000), while with complete SDH inhibition the highest feasible flux values was bounded and ranged between 78 and 123 μmol/(g dry weight × h) (Fig. 2A and B). Upper flux values of the different isoenzymes of the isocitrate dehydrogenase (IDH) reaction were reduced to about 30% or 60% of the flux ranges determined at baseline conditions (Fig. 2A and B). Summed up, the reactions converting isocitrate to alpha-ketoglutarate (AKG) showed a maximum flux capacity between 703 and 902 μmol/(g dry weight × h) at control conditions and between 188 and 261 μmol/(g dry weight × h) for a reaction knockout of succinate dehydrogenase. Flux ranges in the oxidative branch of the pentose phosphate pathway (Phosphogluconate dehydrogenase, PGDH) were reduced to 40% of the baseline flux ranges (upper flux values 205–254 vs. 494–601 μmol/(g dry weight × h) (Fig. 2A) or to 30% when no glucose was supplied as an additional metabolic challenge in the amino acid feed (AA feed) and fatty acid feed (FA feed) scenarios (157–181 vs. 543–554 μmol/(g dry weight × h) (Fig. 2B). Maximum flux capacities of beta-oxidation reactions were reduced to 50–75% at SDH inhibition compared to the control condition (Fig. 2A and B, shown is reaction RCR12716 (palmitoyl-CoA dehydrogenase) as a representative example 298–367 vs. 437–598 μmol/(g dry weight × h)).

For most parts of the intermediary metabolism, including e.g. anaplerotic reactions (e.g. malic enzyme ME, phosphoenolpyruvate carboxykinase PEPCK) and reactions of complex I, III and IV of the respiratory chain (ETC I, III and IV), the impact of an SDH reaction knockout was negligible. Flux ranges were not substantially reduced compared to the baseline condition. No reaction was found to be completely blocked, i.e. not able to carry a flux. Notably, the ATP synthase reaction was neither affected by SDH inhibition, nor by feeding of alternative carbon sources as indicated by identical flux ranges for control conditions, BOS and FLX rat studies (Fig. 2A), and human studies at different feeding test scenarios (GLC, AA feed, FA feed) (Fig. 2B).

3.4.2. Impairment of energy metabolism by simulated complex IV inhibition (e.g. via KCN treatment) causes universal effects on mammalian metabolism

In addition, we compared the flux distributions of a complete SDH inhibition (Fig. 1, scenario 2) with an indisputably more severe metabolic perturbation of the respiratory chain, i.e. inhibition of respiratory chain complex IV, mimicking an intoxication with KCN (Fig. 1, scenario 3). In contrast to the minor effects of SDH inhibition (block of complex II), a block of complex IV resulted in a substantial reduction of flux ranges for most reactions in the rat metabolic network, including fluxes of the central carbon metabolism and energy metabolism, anaplerotic reactions and fatty acid metabolism (Fig. 2C, KCN). The respiratory chain complex III reaction (Fig. 2C, ETC III) was completely blocked and therefore dysfunctional (KCN, 0 μmol/(g dry weight × h)) in contrast to maximum flux values of 586 μmol/(g dry weight × h) for SDH/complex II inhibition (SDH ub 0) and of 720 μmol/(g dry weight × h) at baseline condition (SDH ub 1000). The flux capacity of complex I (Fig. 2C, ETC I) was reduced to 80 μmol/(g dry weight × h) (KCN) compared to upper flux bounds of 552 and 677 μmol/(g dry weight × h) for SDH inhibition (SDH ub 0) and baseline conditions (SDH ub 1000), respectively. Flux capacity of the ATP synthase reaction (Fig. 2C, ATP synthesis) was reduced to 82 μmol/(g dry weight × h) at complex IV inhibition (KCN), while ATP synthesis was neither restricted at baseline conditions (SDH ub 1000) nor at complete SDH inhibition (SDH ub 0).

3.4.3. Partial inhibition of succinate dehydrogenase results in a partial rescue of the baseline metabolic state indicating dose-dependent metabolic effects

The flux distributions of different levels of simulated SDH inhibition allowing fluxes of 1, 10 or 100 μmol/(g dry weight × h) (Fig. 1, scenario 4) were compared to flux ranges resulting from complete SDH inhibition (upper bound 0 μmol/(g dry weight × h)) (Fig. 1, scenario 2) and with the baseline control condition (upper bound 1000 μmol/(g dry weight × h)) (Fig. 1, scenario 1) (Fig. 2C). These simulations were performed with input model 1 (BOS/female/control) for all test conditions (baseline, partial and complete SDH inhibition). A partial inhibition resulted in effects similar to those of complete inhibition of SDH, yet to a lesser extent. In most cases, the flux distributions did not differ between the baseline conditions and an allowed SDH flux of 100 μmol/(g dry weight × h).

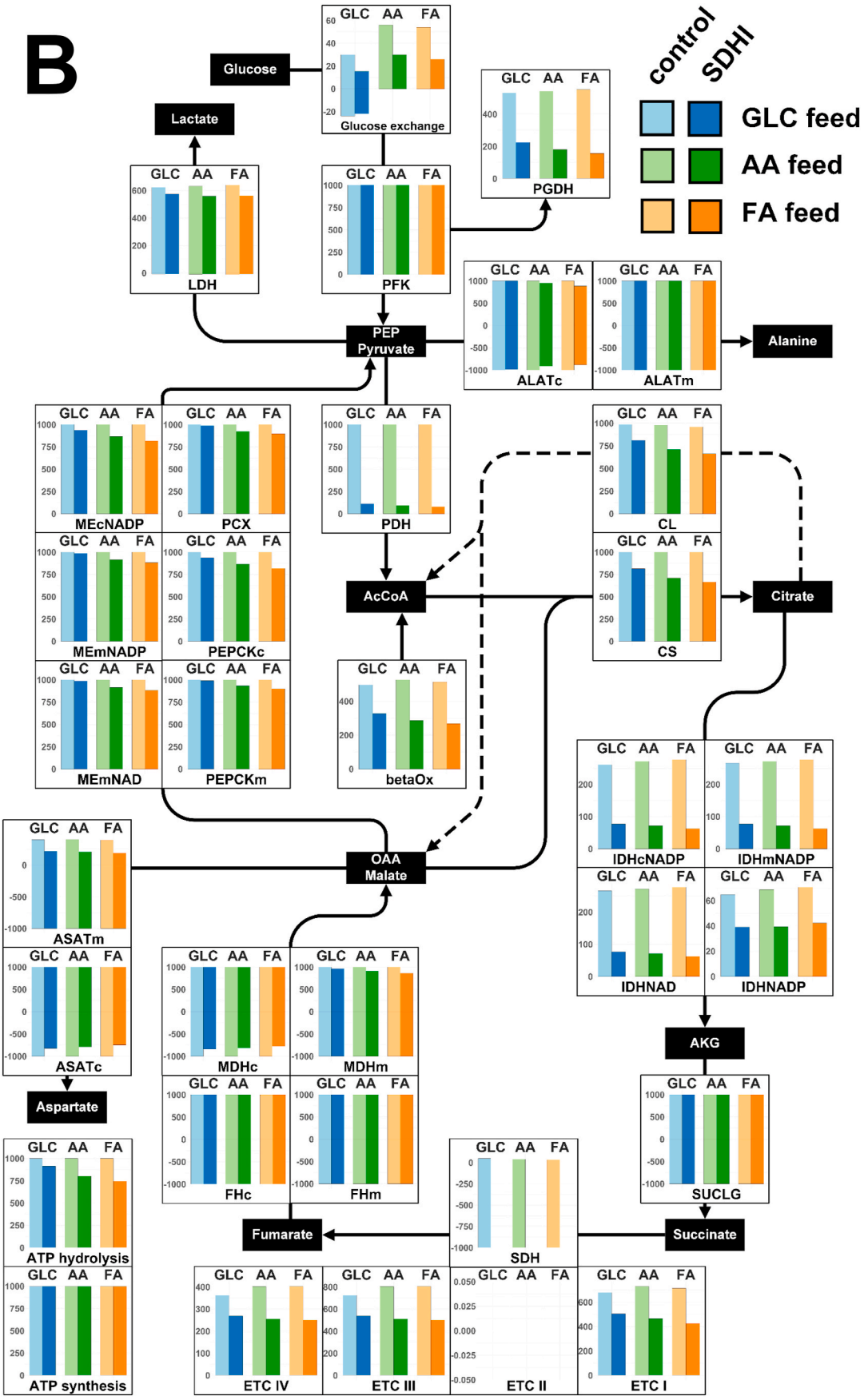

Fig. 2. (*continued*).

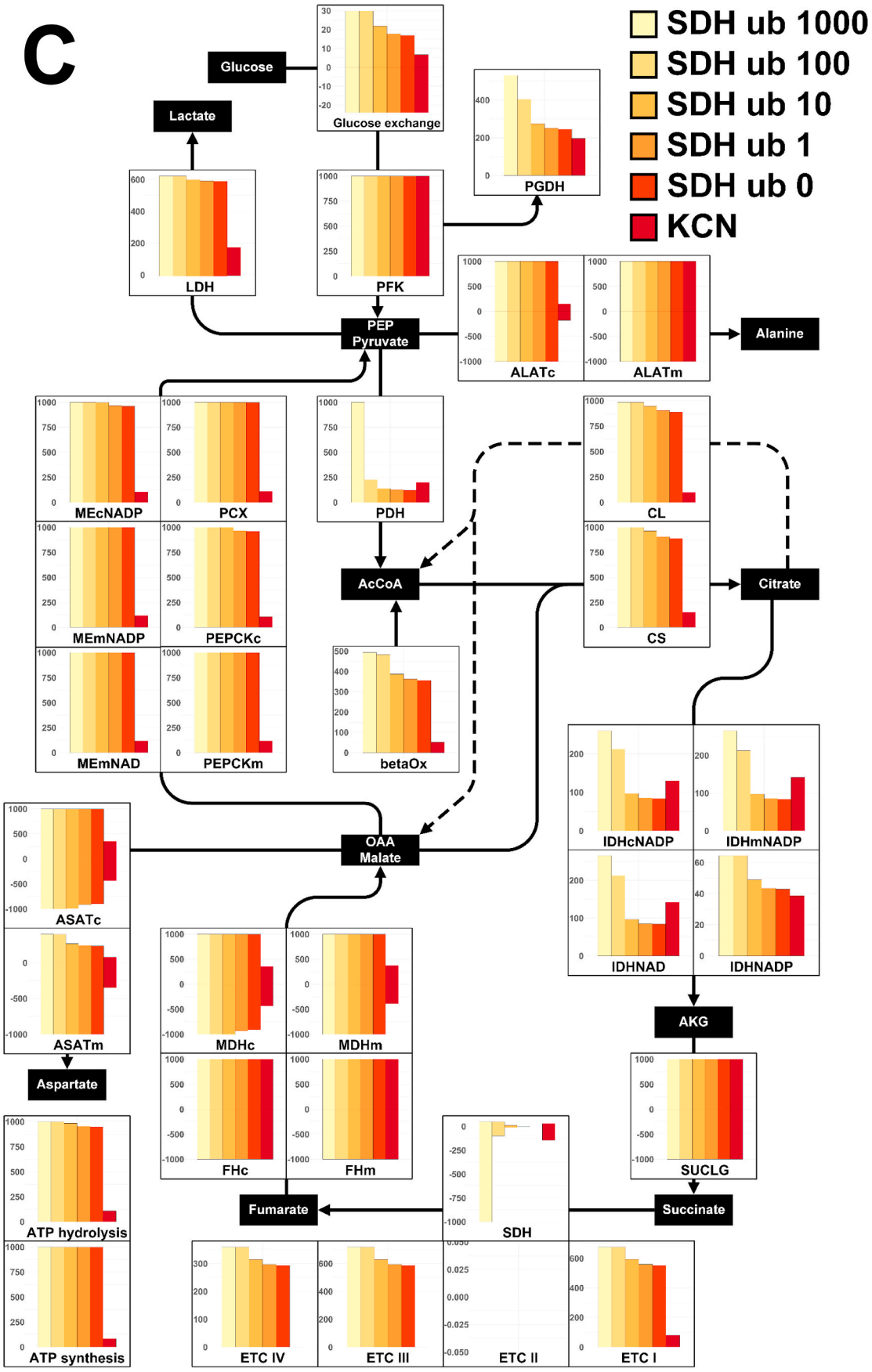

Fig. 2. (*continued*).

3.4.4. The human metabolic network is fully sustained upon SDH inhibition despite glucose deprivation

Only positive values for the glucose exchange flux (Fig. 2, Glucose exchange) were observed in glucose deprived scenarios where amino acids (Fig. 2B, AA feed) or fatty acids (Fig. 2B, FA feed) are fed as major carbon sources, indicating an obligatory glucose excretion when no glucose was available in the feed. In addition, the capacity for glucose excretion was elevated compared to a scenario with glucose supply (Fig. 2B, GLC feed). The metabolic capabilities of the human metabolic network were fully sustained, both at baseline (Fig. 2B, control, scenario 1) and SDH inhibition Fig. 2B, SDHI, scenario 2) conditions, even when no glucose was available in the feed.

4. Discussion

COnstraint-Based Reconstruction and Analysis (COBRA) of genome-scale models can be used to predict the consequences of genetic and environmental perturbations at a systemic level (O'Brien et al., 2015; Gu et al., 2019). We applied comprehensive genome-scale metabolic modeling to evaluate biological capabilities of rat and human to cope with SDH enzyme inhibition. Mammalian metabolism is characterized by network redundancy and the existence of alternative pathways. Flux Variability Analysis (FVA) can quantify this variability by determining the flux boundaries of this feasible range (Orth et al., 2010; O'Brien et al., 2015). The *steady state* flux distributions within this range represent the metabolic capabilities of the target organism at the given constraints and give an indication regarding network flexibility, robustness and vulnerabilities. Constraint-based modeling approaches have limitations. Metabolite concentrations and regulatory effects (e.g. feedback mechanisms, allosteric modifications, etc.) cannot be predicted. Metabolic network reconstructions will inevitably contain knowledge gaps and must be regarded as simplified representations of *in vivo* biological systems (Orth et al., 2010). In our study, the applied experimental data which were imposed as physiological constraints on the models, resulted in wide feasible flux ranges. Therefore, additional constraints (e.g. based on transcriptomics data, quantitative metabolomics data, enzyme assay measurements etc.) will shrink the solution space and allow for more precise predictions based on models that are more specific to the studied condition. However, even an imprecisely known flux space is usually sufficient for comparative analyses and qualitative assessments (O'Brien et al., 2015) and the distinct results obtained for the various different perturbations indicate that the majority of reactions was sensitive to the applied physiological constraints.

We used this *in silico* approach as a computational tool for contextualizing and understanding experimental data from rat as a model organism within the context of human biology. No noticeable differences were found between both species for the metabolic capabilities relevant to the studied effects. The metabolic reconstructions of *Rattus norvegicus* (*iRno*) and *Homo sapiens (iHsa)* used in our study have been specifically created and reconciled for comparative rat versus human metabolism analyses, particularly in the context of systems toxicology applications (Blais et al., 2017). The quality of these reconstructions has been show-cased by accurately capturing known species-specific differences in physiological functions. On the other hand, the highly conserved metabolic functionality between rat and human genome-scale metabolic networks has been highlighted in the original publication as well (Blais et al., 2017). The results of the previous publication together with our findings indicate that the rat is an appropriate test organism for evaluating the toxicity of SDHI fungicides. Transferability of results between rats and humans seem justified for perturbations in the central metabolism.

Metabolic perturbations, such as inhibition of the enzyme SDH, can be simulated *in silico* by restricting flux through the associated reactions. We found that SDH inhibition has only minor effects on the flux distributions in the rat and human metabolic networks. Notably, the absence of any effect on the ATP synthesis function indicates that the energy metabolism is not affected even upon complete SDH inhibition. These findings were rather surprising, given the fact that SDH is a key reaction of central metabolism as part of both the respiratory chain and the TCA cycle. Reduced flux ranges resulting from SDH inhibition were particularly found for decarboxylating reactions (namely pyruvate dehydrogenase, isocitrate dehydrogenase, phosphogluconate dehydrogenase). Based on these observations, one could speculate that SDH inhibition might limit the capabilities for carbon loss in form of CO_2 liberation, forcing the network to operate at a higher carbon-efficiency. A simulated partial inhibition of SDH resulted in similar, yet more moderate effects compared to a complete SDH inhibition, indicating a dose-dependent effect and a partial or in some cases complete restoration of the baseline flux ranges.

In contrast to the moderate effects of SDH inhibition, both in terms of number of affected reactions and severity (extent of flux range reduction), a simulated complex IV inhibition (e.g. as mediated by a KCN intoxication) caused significantly reduced flux ranges for most metabolic reactions, and particularly impaired energy metabolism. The substantial effects observed for the simulated KCN scenario additionally suggest that the applied *in silico* approach is indeed sensitive and sufficient to capture effects induced by metabolic perturbations of the respiratory chain complex.

We found no evidence that the human metabolism is particularly sensitive to SDH inhibition upon glucose deprivation. Our results indicate that the human metabolism can be fully sustained even without glucose intake, solely fed by different alternative carbon sources (amino acids, fatty acids), owing to a fully functional gluconeogenesis with concomitant glucose excretion into the extracellular environment. Therefore, it cannot be excluded that the specific sensitivities observed for the fibroblast cell culture study (Bénit et al., 2019) were an artefact of the *in vitro* experimental setting, while this sensitivity will probably not occur at organism level.

Flux Variability Analysis is often used to determine robustness and flexibility of biochemical reaction networks under different environmental and genetic conditions. The method is used to describe metabolic potential as well as limitations and can elucidate possible metabolic side effects that may not be immediately obvious when considering targeted interventions, such as the inhibition of a single metabolic enzyme, in isolation from the surrounding network. The consideration of metabolic side effects is particularly relevant when metabolic reactions are affected that are interconnected with generic metabolic functions, such as intermediary metabolism, energy generation, or redox balance. Although SDH is a key reaction in mammalian central carbon, redox and energy metabolism, our findings indicate that its inhibition is not expected to have severe effects on the metabolic phenotype. This may be explained by the fact that large-scale mammalian metabolic networks are characterized by a remarkable pathway redundancy, which increases flexibility and sustains fitness of the biological system under varying conditions (O'Brien et al., 2015). We conclude that rat and human metabolism show robustness at various metabolic challenges, including SDH inhibition with or without glucose deprivation. Potential limitations of the TCA cycle can be most likely compensated by various anaplerotic reactions which were not affected by SDH inhibition, and potentially by shifting the metabolic state to a more carbon-efficient operation mode.

The good concordance between the two studies with BOS confirms the robustness and reproducibility of the metabolomics technology employed in these studies, as previously reported by Kamp et al., 2012a, b. This is indicated by the large number of commonly regulated metabolites, but also by the high Pearson correlation coefficient between the two treatments (>99th percentile of all possible correlations in the data base MetaMap®Tox) with no other treatments correlating better. Finally, the common effects identified through the comparison with patterns in the data base MetaMap®Tox shows the similarity of the two BOS treatments.

The *in vivo* plasma metabolome of FLX- and BOS-treated animals

show a significant number of similarities. Both compounds increased the concentration of metabolites related to the fatty acid metabolism and beta-oxidation pathways. Interestingly, the *in silico* analyses revealed a lower maximum capacity for beta-oxidation reactions at SDH inhibition which is consistent with these *in vivo* metabolome findings. In addition, several triacyl-glycerides as well as a few phosphatidyl biosynthesis related metabolites were found at higher levels at FLX- and BOS-treatment. Such changes in fatty acids and complex lipids are often detected in rat studies with compounds that have effects on the liver (e.g., through liver enzyme induction or liver toxicity, van Ravenzwaay et al., 2010). Noteworthy, glucuronic acid was increased consistently for FLX and BOS in both sexes at both dose levels. Glucuronic acid is the precursor of the phase II reaction named glucuronidation which uses activated UDP-glucuronic acid as coupling reagent to increase the excretion of xenobiotic metabolites, but also endogenous compounds such as thyroid hormones (Marquadt et al., 1999). This increase in glucuronic acid is in line with the observation that the plasma metabolome changes of both compounds match with metabolome patterns typical for liver enzyme induction as well as indirect thyroid effects (resulting from increased excretion of thyroid hormones due to liver enzyme induction). Liver enzyme induction has indeed been observed in the repeated oral dose studies in rats conducted with FLX and BOS for regulatory purposes (FAO/WHO 2008, 2013).

As a consequence of SDH inhibition, one would expect changes in energy-related metabolites, especially those involved in the TCA cycle. However, in the plasma metabolome of rats, there were neither consistent effects on malate, citrate and succinate levels in any FLX- and BOS-treated dose group, nor on other energy metabolism-related metabolites, such as pyruvate or lactate. Overall, the changes relative to controls of these metabolites were low and mostly not statistically significant. Furthermore, neither a dose-response relationship, nor consistency between the sexes was observed. In the case of the two studies with BOS, effects on these metabolites were not reproducible. Thus, with respect to the fungicide mode of action of both compounds – SDH inhibition – which plays a prominent role in the TCA cycle and the interconnected electron transport chain, there was an absence of any consistent change in any of the treatment groups, indicating a fully functional TCA cycle in the mitochondria. This is in line with the results from our *in silico* approach. In *in vitro* experiments carried out by Bénit et al. (2019) observed reduced cell viability in response to SDHI fungicide exposure, = was considered by the authors to reflect mitochondrial toxicity. However, such effects were obtained only under cell culture conditions that prevented glycolysis (using cell culture medium that lacked glucose, pyruvate and uridine and contained glutamine as sole carbon source). These exposure conditions and scope of investigations differed in important aspects from recently published cell culture experiments of the EU-ToxRisk project, which investigated the effects of mitochondrial targeting agrochemicals, including five SDH inhibitors, on HepG2 and RPTEC/TERT1 cells using a battery of tests (van der Stel et al., 2020). The tested Complex II inhibitors had no notable effects on viability, lactate production, mitochondrial membrane potential, extracellular acidification and oxygen consumption rates in intact cells exposed for 24 h to up to 10 μM of the investigated chemicals. Exposures were carried out either in the presence of glucose or using galactose as replacement. The absence of notable mitochondrial toxicity by Complex II inhibitors, with no evidence for decreased ATP production, evidence for lactate accumulation or lactate acidosis, are fully in line with the scenario outcome predictions of our *in silico* analyses that considered complete or partial inhibition of SDH in the absence of glucose supply, and to the results of the metabolome profile of rats following exposure up to 28 days to the SDH inhibitors boscalid and fluxapyroxad.

Results of respiration and membrane potential assays as reported (van der Stel et al., 2020) indicated a slight (non-significant) tendency of compensatory mechanisms at complex II inhibition and we also contained hints of compensation effects. We observed higher plasma levels of several amino acids in our *in vivo* metabolome studies. Different amino acids such as branched chain amino acids or threonine can be catabolized to succinyl-CoA and feed carbons into the TCA cycle (Michal and Schomburg, 2012). Higher plasma levels found for isoleucine, valine and threonine at BOS and FLX treatment compared to controls suggest that carbon input at the point of succinate/succinyl-CoA into the TCA cycle is controlled by reducing the expensive catabolism of these essential amino acids. 2-hydroxy butyrate, a side product of threonine degradation, was found to be consistently decreased through treatment with FLX and BOS, supporting this hypothesis. In addition, the results of the *in silico* analysis also hint at a compensation mechanism by shifting the metabolism to higher efficiency as explained above.

The multitude of different pathways and cellular functions where succinate is involved requires holistic approaches to study SDHI effects, such as genome-wide metabolic modeling or *in vivo* studies. Recent studies reviewing the multifaceted roles of succinate as a metabolite and signaling molecule additionally highlight the fact that dynamic ranges of both SDH activity and succinate levels are physiological and influenced by various conditions (Guo et al., 2020; Tretter et al., 2016). This explains the high metabolic flexibility to adjust for changes in succinate and SDH activity levels.

A sound basis for extrapolating expected effects in humans from rodent toxicity studies is provided by complementary approaches that combine (1) SDHI-induced *in vivo* metabolome changes in rats, (2) comparison of SDH inhibition effects in both rat and human metabolism *in silico*, as well as (3) different what-if scenarios tested *in silico* to describe the range of flexibility and limitations in mammalian metabolic networks.

Due to the reconciliation of the rat and human metabolic models it is possible to compare the responses to SDH inhibition of rat and human *in silico*. As no noticeable differences were found between both species, the rat appears to be an appropriate test organism for toxicity of SDHIs.

In conclusion, the *in vivo* analysis indicated that fungicidal mode of action of both compounds, i.e. inhibition of SDH activity, does not result in a notable change in succinate or lactate levels. The most likely reason for this is, as shown in the flux variability analysis, the existence of multiple biochemical pathways that can substitute for reduced SDH activity and maintain biochemical homeostasis.

Credit author statement

H. Kamp: methodology, formal analysis, investigation, writing – original draft, visualization.

J. Wahrheit: methodology, software, formal analysis, data curation, writing – original draft, visualization.

S. Stinchcombe: conceptualization, writing – original draft, review & editing.

T. Walk: formal analysis, investigation, data curation, writing – review & editing

F. Stauber: conceptualization, writing – review & editing.

B. v. Ravenzwaay: conceptualization, formal analysis, writing – review & editing, supervision.

Declaration of competing interest

All authors declare the following financial interests/personal relationships which may be considered as potential competing interests: The authors are employees of BASF, a chemical company developing, producing and marketing chemicals including SDHI compounds. Dr. Wahrheit is an employee of BASF, a chemical company developing, producing and marketing chemicals including SDHI compounds.

Acknowledgements

This work has been funded by BASF.

Appendix A. Supplementary data

Supplementary data to this article can be found online at https://doi.org/10.1016/j.fct.2021.112085.

References

Bénit, P., Kahn, A., Chretien, D., Bortoli, S., Huc, L., Schiff, M., Gimenez-Roqueplo, A.-P., Favier, J., Gressens, P., Rak, M., et al., 2019. Evolutionarily conserved susceptibility of the mitochondrial respiratory chain to SDHI pesticides and its consequence on the impact of SDHIs on human cultured cells. PloS One 14, e0224132. https://doi.org/10.1371/journal.pone.0224132.

Blais, E.M., Rawls, K.D., Dougherty, B.V., Li, Z.I., Kolling, G.L., Ye, P., Wallqvist, A., Papin, J.A., 2017. Reconciled rat and human human metabolic networks for comparative toxicogenomics and biomarker predictions. Nat. Commun. 8, 14250. https://doi.org/10.1038/ncomms14250.

FAO/WHO, 2008. Food and agriculture organization of the united nations, world health organization, FAO panel of experts on pesticide residues in food and the environment & WHO core assessment group on pesticide residues. In: (2008). Pesticide Residues in Food : 2006, Toxicological Evaluations, Sponsored Jointly by FAO and WHO, with the Support of the International Programme on Chemical Safety, Joint Meeting of the FAO Panel of Experts on Pesticide Residues in Food and the Environment and the WHO Core Assessment Group, Rome, Italy, 3-12 October 2006. World Health Organization. Part 2, Toxicological. https://apps.who.int/iris/handle/10665/43822.

FAO/WHO, 2013. FAO Panel of Experts on Pesticide Residues in Food and the Environment, WHO Core Assessment Group on Pesticides Residues & Joint Meeting of the FAO Panel of Experts on Pesticide Residues in Food and the Environment and the WHO Core Assessment Group on Pesticide Residues, Rome, Italy, 11-20 September 2012. Pesticide residues in food - 2012: toxicological evaluations. World Health Organization, 2013. https://apps.who.int/iris/handle/10665/85391.

Gu, C., Kim, G.B., Kim, W.J., Kim, H.U., Lee, S.Y., 2019. Current status and applications of genome-scale metabolic models. Genome Biol. 20 (1), 121. https://doi.org/10.1186/s13059-019-1730-3.

Guo, Y., Cho, S.W., Saxena, D., Li, X., 2020. Multifaceted actions of succinate as a signaling transmitter vary with its cellular locations. Endocrinol. Metab. (Seoul) 35 (1), 36–43. https://doi.org/10.3803/EnM.2020.35.1.36.

Hederstedt, L., 2003. Complex II is complex too. Science 299, 671. https://doi.org/10.1126/science.1081821.

Heirendt, L., Arreckx, S., Pfau, T., Mendoza, S.N., Richelle, A., Heinken, A., Haraldsdóttir, H.S., Wachowiak, J., Keating, S.M., Vlasov, V., et al., 2019. Creation and analysis of biochemical constraint-based models using the COBRA Toolbox v.3.0. Nat. Protoc. 14 (3), 639–702. https://doi.org/10.1038/s41596-018-0098-2.

Kamp, H., Fabian, E., Groeters, S., Herold, M., Krennrich, G., Looser, R., Mattes, W., Mellert, W., Prokoudine, A., Ruiz-Noppinger, P., 2012a. Application of in vivo metabolomics to preclinical/toxicological studies: case study on phenytoin-induced systemic toxicity. Bioanalysis 4, 2291–2301. https://doi.org/10.4155/bio.12.214.

Kamp, H., Strauss, V., Wiemer, J., Leibold, E., Walk, T., Mellert, W., Looser, R., Prokoudine, A., Fabian, E., Krennrich, G., et al., 2012b. Reproducibility and robustness of metabolome analysis in rat plasma of 28-day repeated dose toxicity studies. Toxicol. Lett. 215, 143–149.

Koziel, A., Jarmuszkiewicz, W., 2017. Hypoxia and aerobic metabolism adaptations of human endothelial cells. Pflugers Arch. 469, 815–827. https://doi.org/10.1007/s00424-017-1935-9.

Lewis, N.E., Nagarajan, H., Palsson, B.O., 2012. Constraining the metabolic genotype-phenotype relationship using a phylogeny of in silico methods. Nat. Rev. Microbiol. 10 (4), 291–305. https://doi.org/10.1038/nrmicro2737.

Lindon, J.C., Holmes, E., Nicholson, J.K., 2004. Toxicological applications of magnetic resonance. Prog. Nucl. Magn. Reson. Spectrosc. 45, 109–143.

Marquardt, H., Schäfer, S., McClellan, R.O., Welsch, F., 1999. Toxicology, Academic Press. Hardcover, first ed., ISBN 9780124732704 eBook ISBN: 9780080543116.

Mattes, W., Davis, K., Fabian, E., Greenhaw, J., Herold, M., Looser, R., Mellert, W., Groeters, S., Marxfeld, H., Moeller, N., et al., 2014. Detection of hepatotoxicity potential with metabolite profiling (metabolomics) of rat plasma. Toxicol. Lett. 230, 467–478. https://doi.org/10.1016/j.toxlet.2014.07.021.

Mattes, W.B., Kamp, H.G., Fabian, E., Herold, M., Krennrich, G., Looser, R., Mellert, W., Prokoudine, A., Strauss, V., van Ravenzwaay, B., 2013. Prediction of clinically relevant safety signals of nephrotoxicity through plasma metabolite profiling. BioMed Res. Int. 202497. https://doi.org/10.1155/2013/202497, 2013.

Mellert, W., Kapp, M., Strauss, V., Wiemer, J., Kamp, H., Walk, T., Looser, R., Prokoudine, A., Fabian, E., Krennrich, G., et al., 2011. Nutritional impact on the plasma metabolome of rats. Toxicol. Lett. 207, 173–181.

Michal, G., Schomburg, D., 2012. Biochemical Pathways: an Atlas of Biochemistry and Molecular Biology. John Wiley & Sons/Wiley John + Sons.

Montoya, G.A., Strauss, V., Fabian, E., Kamp, H., Mellert, W., Walk, T., Looser, R., Herold, M., Krennrich, G., Peter, E., et al., 2014. Mechanistic analysis of metabolomics patterns in rat plasma during administration of direct thyroid hormone synthesis inhibitors or compounds increasing thyroid hormone clearance. Toxicol. Lett. 225, 240–251. https://doi.org/10.1016/j.toxlet.2013.12.010.

O'Brien, E.J., Monk, J.M., Palsson, B.O., 2015. Using genome-scale models to predict biological capabilities. Cell 161 (5), 971–987. https://doi.org/10.1016/j.cell.2015.05.019.

Orth, J.D., Thiele, I., Palsson, B.Ø., 2010. What is flux balance analysis? Nat. Biotechnol. 28 (3), 245–248. https://doi.org/10.1038/nbt.1614.

Price, N.D., Reed, J.L., Palsson, B.Ø., 2004. Genome-scale models of microbial cells: evaluating the consequences of constraints. Nat. Rev. Microbiol. 2 (11), 886–897. https://doi.org/10.1038/nrmicro1023.

Strauss, V., Wiemer, J., Leibold, E., Kamp, H., Walk, T., Mellert, W., Looser, R., Prokoudine, A., Fabian, E., Krennrich, G., et al., 2009. Influence of strain and sex on the metabolic profile of rats in repeated dose toxicological studies. Toxicol. Lett. 191, 88–95.

Rasheed, M., Tarjan, G., 2018. Succinate dehydrogenase complex: an updated review. Arch. Pathol. Lab Med. 142, 1564–1570. https://doi.org/10.5858/arpa.2017-0285-RS.

Roessner, U., Wagner, C., Kopka, J., Trethewey, R., Willmitzer, L., 2000. Technical advance: simultaneous analysis of metabolites in potato tuber by gas chromatography-mass spectrometry. Plant J. 23, 131–142. https://doi.org/10.1046/j.1365-313x.2000.00774.x.

Strauss, V., Mellert, W., Wiemer, J., Leibold, E., Kamp, H., Walk, T., Looser, R., Prokoudine, A., Fabian, E., Krennrich, G., et al., 2012. Increased toxicity when fibrates and statins are administered in combination–a metabolomics approach with rats. Toxicol. Lett. 211, 187–200. https://doi.org/10.1016/j.toxlet.2012.03.798.

Suckow, M., Weisbroth, S., Franklin, C., et al., 2006. In: Suckow, M., Franklin, C., Weisbroth, S. (Eds.), The Laboratory Rat, Second Edition. Academic Press.

Tretter, L., Patocs, A., Chinopoulos, C., 2016. Succinate, an intermediate in metabolism, signal transduction, ROS, hypoxia, and tumorigenesis. Biochim. Biophys. Acta 1857, 1086–1101.

van Ravenzwaay, B., Cunha, G.C.-P., Leibold, E., Looser, R., Mellert, W., Prokoudine, A., Walk, T., Wiemer, J., 2007. The use of metabolomics for the discovery of new biomarkers of effect. Toxicol. Lett., Biomark. Children Adults 172, 21–28. https://doi.org/10.1016/j.toxlet.2007.05.021.

van der Stel, W., Carta, G., Eakins, J., Darici, S., Delp, J., Forsby, A., Bennekou, S., Gardner, I., Leist, M., Danen, E., Walker, P., van der Water, B., Jennings, P., 2020. Multiparametric assessment of mitochondrial respiratory inhibition in HepG2 and RPTEC/TERT1 cells using a panel of mitochondrial targeting agrochemicals. Arch. Toxicol. 94, 2707–2729. https://doi.org/10.1007/s00204-020-02792-5.

van Ravenzwaay, B., Coelho-Palermo Cunha, G., Fabian, E., Herold, M., Kamp, H., Krennrich, G., Krotzky, A., Leibold, E., Looser, R., et al., 2010. The use of metabolomics in cancer research. In: Cho, W.C.S. (Ed.), An Omics Perspective of Cancer. Springer Science + Media B.V., Dordrecht, pp. 141–166.

van Ravenzwaay, B., Herold, M., Kamp, H., Kapp, M.D., Fabian, E., Looser, R., Krennrich, G., Mellert, W., Prokoudine, A., et al., 2012. Metabolomics: a tool for early detection of toxicological effects and an opportunity for biology based grouping of chemicals-from QSAR to QBAR. Mutat. Res. 746, 144–150. https://doi.org/10.1016/j.mrgentox.2012.01.006.

van Ravenzwaay, B., Kamp, H., Montoya, G.A., Strauss, V., Fabian, E., Mellert, W., Krennrich, G., Walk, T., Peter, E., Looser, R., et al., 2015. The development of a database for metabolomics – looking back on ten years of experience. Int. J. Biotechnol. 14 (1).

Viant, M., Ebbels, T., Beger, R., Ekman, D., Epps, D., Kamp, H., Leonards, P., Loizou, G., MacRae, J., van Ravenzwaay, B., Rocca-Serra, P., Salek, R., Walk, T., Weber, R., 2019. Best practice and reporting standards for applications of metabolomics in regulatory toxicology. Nat. Commun. 10 https://doi.org/10.1038/s41467-019-10900-y. Article No. 3041.